The Tissue Distribution of Tumor Necrosis Factor-α in Rats: A Compartmental Model

Mary Keith, Kenneth H. Norwich, Willy Wong, and Khursheed N. Jeejeebhoy

Tumor necrosis factor (TNF) is widely accepted to be the mediator of the cascade of metabolic abnormalities associated with both critical and chronic illness. TNF binding to cell surface receptors mediates its physiologic actions, although the exact mechanism of TNF action is unknown. Therefore, this study was designed to investigate the in vivo metabolism of TNF using a mathematical model to examine tissue uptake and loss of TNF over time. Two distinct patterns of TNF uptake were observed. Muscle tissues were found to accumulate TNF over the entire experimental period, whereas the visceral organs were found to have a rapid initial accumulation of TNF followed by a rapid loss of TNF back to the plasma or out into the bile or the urine. These patterns of TNF binding and retention may reflect the number of TNF receptors or their affinity for TNF, as well as the balance between cell surface and soluble TNF receptors. Furthermore, TNF binding patterns provide insight into the biologic action of TNF at these sites.

CHRONIC PRODUCTION of tumor necrosis factor (TNF) has been associated with the wasting observed in both critical and chronic illness in humans, such as in acquired immune deficiency syndrome (AIDS), sepsis, or cancer. The wasting of vital body proteins may ultimately affect survival. Acute overexpression of TNF results in hemodynamic collapse with hypotension, decreased vascular resistance, and organ failure.[1] The production of TNF initiates a cascade of endogenous mediators including interleukin (IL)-1 and IL-6, which amplify and modulate many of the systemic effects of TNF.[1] In addition, the binding of TNF to its 2 distinct cell surface receptors, p-55 and p-75, has also been shown to be necessary for TNF to exert its physiologic effects.[2] We and others have previously described the uptake of TNF by tissues at a single point in time.[3-6] However, while TNF binding to cell surface receptors has been studied in vitro, the distribution and fate of circulating TNF has not been studied in detail. Therefore, this study was designed to examine the distribution of TNF in vivo by using a compartmental model to describe the movement of TNF between the plasma and the tissues over a 3-hour experimental period. The binding patterns of TNF may provide insight into the physiologic actions of TNF at each tissue. This study represents a portion of a study designed to determine whether the route or the nutrient density of nutrition support will affect the distribution pattern of TNF.

MATERIALS AND METHODS

Animals

Male Wistar rats (Charles River Canada, Quebec, Canada) were individually housed in cages at a temperature of 22°C and maintained on a 12-hour light:dark cycle. Rats on entry to the animal facility weighed 200 to 220 g. All animals were maintained on a diet of laboratory food ad libitum until they achieved a weight of 240 to 260 g. Under general anesthesia (sodium pentobarbital, 50 mg/kg intraperitoneal [IP]) a Silastic catheter (0.037 in OD, Dow Corning, Midland, MI) was inserted and advanced into the superior vena cava using the sterile procedure of Popp and Brennan,[7] which is described in detail elsewhere.[5] The external portion of the catheter was tunnelled subcutaneously to the interscapular region of the back and led externally through a protective wire spring and secured to the rat by a stainless steel button (Instech Labs, Horsham, PA). Postoperatively, the rats were housed in individual metabolic cages and maintained on a specially formulated liquid diet given orally ad libitum. Animals had free access to drinking water during the entire experimental procedure. Patency of the catheter was maintained by a daily injection of 0.5 mL of heparinized saline (sodium heparin, 10 U/mL) into the catheter.

Diet Formulation

All animals were provided with a specially formulated liquid diet. The composition of the diet has been described previously in detail.[5,8] Briefly, it is a high carbohydrate diet with 72% of the energy provided coming from carbohydrate sources, 13% of energy from protein (amino acids), and 15% of energy from fat. The nutrients infused met the macronutrient requirements for rats, and previous trials have shown that this diet allowed control rats to grow at the same rate as chow-fed animals.[5,8] Animals received on average 79.0 kcal/d and 0.4 g N per day (nonprotein energy:nitrogen ratio of 183.8).

Study Protocol

On day 0 of experimentation, the catheter and spring were connected to a swivel device (Instech Labs), which allowed movement of the animal about the cage. The swivel device was suspended above the metabolic cage by a metal rod. Rats in this portion of the study were maintained on an ad libitum oral intake of the defined liquid diet. Physiologic saline was aseptically placed in 60-mL syringes (Becton-Dickinson, Rutherford, NJ) and continuously infused by an infusion pump at a rate of 2.5 cc/h (pump 22; Harvard Apparatus, Wellesley, MA).

After 5 days of saline infusion, rats were anaesthetized with an injection of 25 mg/kg sodium pentobarbital intraperitoneally. Saline infusion and an oral diet were continued until the time of study with no animal being maintained without nutrition for a period of longer than 60 minutes before experimentation. A bolus of 100 mg of sodium iodide was given to block uptake of radioactive iodine by the thyroid. After this, 200 µL of labeled red blood cells were injected and allowed to distribute for 10 minutes. Chromium-labeled blood was prepared in advance using red blood cells from separate rats as described below. A

From the Departments of Nutrition, Physiology, and Physics and the Institute of Biomaterials and Biomedical Engineering, University of Toronto, Toronto, Canada.

Submitted October 21, 1999; accepted April 9, 2000.

Supported by Medical Research Council Operating Grant No. MT-12238, and by the Natural Sciences and Engineering Research Council.

Address reprint requests to Mary Keith, PhD, 3 Queen 3-080, St. Michael's Hospital, 30 Bond St, Toronto, Ontario M5B 1W8.

0026-0495/00/4910-0020$10.00/0

doi:10.1053/meta.2000.9525

sample of 200 µL of red blood cells was counted as a standard injected dose of chromium. A sample of 0.3 mL of blood was collected into a heparinized syringe for hematocrit determination, as well as for analysis of radioactive chromium in order to determine blood volume.

The abdomen was subsequently opened, and the bile duct and the bladder were cannulated for the collection of bile and urine. A lamp was maintained over the animals to maintain body temperature under anaesthetic. Catheters were preinjected with 0.5 mL of 2% bovine serum albumin to coat the lumen of the tube, thereby preventing adherence of radioactive material to the lumen of the cannula. Subsequently, a bolus of 0.3 µCi of ^{125}I-TNF ([^{125}I] iodotyrosyl TNF-α, Amersham Canada, Oakville, Ontario) together with 0.5 µg of unlabeled TNF-α (Upstate Biotechnology, Lake Placid, NY) were injected via the central venous catheter. Previous studies indicated that the injection of either human or rat TNF at this dose did not result in any significant changes in either blood pressure or heart rate measured at the time of TNF injection or throughout the 3-hour experimental period. Blood samples were withdrawn from the central venous catheter into heparinized syringes at exact timed intervals noted in a computer stop watch program. For each experimental group, a duplicate aliquot of the injected dose was kept as a standard. At each time point, 0.3 mL of blood was taken and the catheter flushed with 0.3 mL of 0.9% saline. The experiment was terminated at 5 different time points postinjection of labeled TNF and 10 tissues and organs were collected for analysis of radioactivity as outlined above. Rats were killed at 4, 10, 30, 60, and 180 minutes post-TNF injection by an overdose of sodium pentobarbital given through the central venous catheter. Death was instantaneous, however, the chest cavity was immediately opened and the aorta severed to prevent any further blood flow to the tissues. The liver, spleen, lungs, kidneys, heart, extensor digitorum longus (EDL), soleus, diaphragm, stomach, and intestine were dissected and weighed. The radioactivity present in the skeletal muscle was estimated using the percentage of body weight that is skeletal muscle and the mean uptake of TNF by the EDL. Bile and urine collected over the experimental period were analyzed for radioactivity. The results represent the average uptake of approximately 5 to 6 animals per feeding group at each of the 5 time points post-TNF injection, resulting in data being available for approximately 25 animals. Organ uptake data was corrected for residual blood present in the tissue using the radioactivity measured as chromium. The mean of each group of animals for each time point was calculated.

A separate group of 6 rats was studied to collect information on the uptake of TNF by the skin and adipose tissue. Skin samples were collected from the abdominal area and adipose tissue that was located in the abdominal cavity surrounding the spine and the kidneys. In these animals we also followed the release of radioactivity into the bile and the urine over the entire 3-hour period as the pooled results from our initial work were difficult to interpret due to large variations in bile and urine collection.

Tumor Necrosis Factor-α

Recombinant human TNF was obtained from Upstate Biotechnology. The endotoxin content was less than 25 ng lipopolysaccharide/mg TNF (according to the product specifications). The TNF was diluted according to the manufacturer's instructions and stored at −70°C as 2-mL aliquots each containing 25 µg of TNF. Labeled TNF was purchased from Amersham Canada (Oakville, Ontario) with a specific activity of 400 to 800 mCi/mmol.

To evaluate the proportion of active TNF in the samples, separate experiments were conducted in which a bolus of labeled TNF alone was injected into a rat and the blood collected immediately after injection, as well as after circulating for a 3-hour period. These plasma samples were separated and precipitated with 15% trichloracetic acid. The precipitate was redissolved in NaOH and subjected to high performance liquid chromatography (HPLC) separation on a C-4 protein column (Waters, Mississauga, Ontario) according to the method of Gutierrez et al.[9] In addition, HPLC separation of the native ^{125}I-TNF was performed. Finally, a sample taken from each HPLC peak was subjected to sodium dodecyl sulfate-polyacrylamide gel electrophoresis (SDS-PAGE) according to the method of Laemmli[10] and adapted by Raina et al.[11] Briefly, samples were subjected to electrophoresis in the presence of 10% SDS on a 4% to 15% acrylamide gradient gel at a constant current of 25 mA. SDS gels were prepared without the addition of mercaptoethanol or dithiothreitol (ddt), thereby allowing the various forms of TNF to be viewed.[11]

Chromium Labeling of Red Blood Cells

Red blood cells from a separate group of animals were incubated with radioactive chromium (Amersham Canada, specific activity 250 to 500 mCi/mg Cr) as $Na_2Cr_{51}O_4$ for 1 hour at 37°C. Subsequently, the cells were washed twice with cold normal saline, once with 10 nmol/L ascorbic acid, and twice more with saline. A stock solution of chromium was used to correct for chromium measured in the iodine channel.

On the day of experimentation, rats were injected with 300 µL of labeled red blood cells through the central venous catheter. A 10-minute distribution time was found to be adequate by Sterling and Gray.[12] At this time, blood was collected through the central venous catheter for the measurement of radioactivity, according to the method above for whole blood, as well as for the calculation of the hematocrit. The dilution of the dose of labeled red blood cells allowed the calculation of blood volume.

Measurement of Radioactivity in Whole Blood, Bile, and Urine

A sample of 100 µL of whole blood was placed in 12 × 75 glass tubes for gamma counting. The pipette tip was rinsed with 0.9% saline to ensure that all of the blood was removed. The protein was precipitated with 1.5 mL of 15% trichloroacetic acid (TCA), centrifuged at 3,000 rpm for 5 minutes and the supernatant removed and discarded. This process was repeated to ensure optimal removal of the non–protein-bound radioactivity. The remaining pellet was dissolved in 1.5 mL of 3N NaOH and counted for radioactivity in a dual channel gamma counter (Beckman Gamma 5500, Beckman Instruments, Irvine, CA).

Samples of 100 µL of bile and urine were placed in 12 × 75 glass tubes and analyzed for radioactivity before precipitation. The volume of bile and urine collected was also measured and recorded. After initial radioactivity analysis, bile and urine samples were precipitated with 15% TCA and spun for 5 minutes at 3,000 rpm. The supernatant was removed and the pellet was dissolved in 3 N NaOH and counted for radioactivity.

Measurement of the Uptake of ^{125}I-TNF by Organs

Organ samples were homogenized with normal saline followed by precipitation with 1.5 mL of 15% TCA. Precipitated samples were centrifuged for 5 minutes at 3,000 rpm, and the supernatant was subsequently removed and discarded. This procedure was repeated once to ensure the removal of any nonprotein-bound radioactivity. The pellet was dissolved in 1.5 mL 10 N NaOH for 24 hours and counted for radioactivity as described above.

The presence of radioactive chromium in the tissues allowed the samples to be corrected for any residual blood content. A stock sample of chromium solution was counted to determine the percentage of the radioactivity that was counted in the iodine channel. The calculation for the tissue uptake of labelled TNF was as follows: Net ^{125}I counts in tissue sample = [^{125}I counts in sample(cpm) − background ^{125}I counts (cpm)] − [^{51}CR counts (cpm) in sample − background ^{51}CR counts (cpm)] × % of ^{51}CR spillover into the ^{125}I channel. The weight of the tissue sample counted was then used to calculate the uptake of the organ on a per gram or total organ basis.

Gel Electrophoresis

A tricine SDS-PAGE system for small proteins was used for the separation of bile and urine. The method used was designed for the

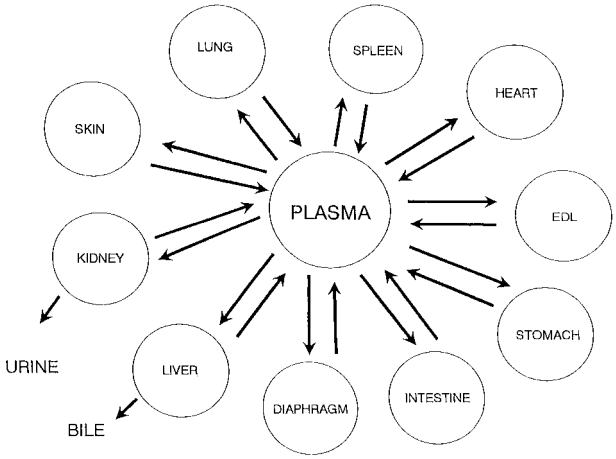

Fig 1. A mammillary compartmental model. This model describes the interaction of TNF between the plasma and each of the 10 organs and tissues examined with the irreversible loss of material into the bile and the urine.

separation of low-molecular weight proteins (1 to 100 kD) and was based on the method of Laemmli.[10,13]

COMPARTMENTAL MODELING OF ORGAN UPTAKE DATA

Formulating the Model

TNF was injected as a bolus into the plasma and was subsequently distributed into many body tissues. Since the plasma volume was known, the total mass of TNF remaining in plasma could be estimated from measurements of plasma TNF concentration. TNF mass in 10 types of tissue was assessed. Measurements of TNF mass were made 5 times in each of the 10 tissues. The kinetics of TNF were modeled using a multicompartment model in a mamillary configuration, with plasma exchanging material reversibly with each of the 10 peripheral compartments. One of the peripheral compartments, liver, exchanged material reversibly with plasma and lost material irreversibly to bile. Another peripheral compartment, kidney, exchanged reversibly with plasma and lost irreversibly to urine. This model is depicted in Fig 1.

There is one differential equation for each of the 11 compartments and 2 others to account for irreversible loss. We shall designate by $M_P(t)$ the mass of TNF in plasma at time, t; by $M_S(t)$ the mass of TNF in spleen, by $M_R(t)$ the mass in kidney, $M_L(t)$ the mass in liver, etc. The rate constants, whose dimensions are time^{-1}, are designated by Ks, where K_{PS} governs transfer of TNF from spleen to plasma, etc. The 11 primary differential equations are of the form:

$$\frac{dM_P}{dt} = -(K_{SP} + K_{RP} + K_{LP} + \ldots) M_P + K_{PS} M_S + K_{PR} M_R + K_{PL} M_L + \ldots \quad (1)$$

$$\frac{dM_S}{dt} = K_{SP} M_P - K_{PS} M_S \quad (2)$$

$$\frac{dM_R}{dt} = K_{RP} M_P - (K_{PR} + K_{UR}) M_R \quad (3)$$

$$\frac{dM_L}{dt} = K_{LP} M_P - (K_{PL} + K_{BL}) M_L \quad (4)$$

. . .

where K_{UR} and K_{BL} designate the rate constants governing exchange between kidney and urine and between liver and bile, respectively. The 2 remaining differential equations governing irreversible loss are of the form given by equation (9) below. For a general peripheral compartment, X, we can write:

$$\frac{dM_X}{dt} = K_{XP} M_P - K_{PX} M_X, \quad (5)$$

where X stands for S, R, L, etc. Because initially there is no TNF in peripheral compartment X, we can solve the latter equation for M_X in terms of M_P:

$$M_X(t) = K_{XP}\, e^{-K_{PX}t} \int_0^t e^{K_{PX}t} M_P(t)\, dt \quad (6)$$

Estimating the Rate Constants

The rate constants were determined from the measured data. After the bolus injection of TNF into plasma, the plasma concentration of TNF fell, approximately monotonically, and was fitted to the sum of 3 real, negative exponentials of the form:

$$M_P = A_1 e^{-\beta_1 t} + A_2 e^{-\beta_2 t} + A_3 e^{-\beta_3 t} \quad (7)$$

where the As and βs are greater than zero. Each of the 10 peripheral compartments that exchanged material with plasma were governed by a differential equation of the form of equation (5). Because M_P was known as a function of time from equation (7), this function was introduced into the integral on the right-hand side of equation (6). The resulting equation then gives $M_X(t)$ as a function of time governed by 2 unknown rate constants, K_{XP} and K_{PX}. The measured data for peripheral compartment X were then curve-fitted to this function, thus providing values for the 2 unknown rate constants. This procedure was repeated for each of the 10 interchanging peripheral compartments.

In the case of the liver and kidney compartments, the rate constant K_{PX} was really the sum of 2 rate constants, one governing return of TNF to plasma, and the other governing irreversible loss of TNF to bile or urine. For the liver compartment we have, with reference to equation (4):

$$K_{\Sigma L} = K_{PL} + K_{BL}. \quad (8)$$

However, it was a straightforward matter to estimate the value of K_{BL} using the biliary data. Because TNF passed irreversibly from liver into bile, its kinetics were described by the differential equation:

$$\frac{dB}{dt} = K_{BL} M_L, \quad (9)$$

where $B(t)$ represents the mass of TNF in bile at time, t. This equation may be integrated to give:

$$B(t) = K_{BL} \int_0^t M_L\, dt. \quad (10)$$

From the measured TNF masses in both liver and bile, we were able to estimate a value for the rate constant, K_{BL}. Because we had a value for the constant $K_{\Sigma L}$, we could solve for the remaining rate constant, K_{PL} using equation (8). In a similar manner, we were able to obtain a value for K_{PR} and K_{UR}. Therefore, all rate constants could be determined.

Curve-fitting was performed with a simplex algorithm using the least squares criterion. Data points were usually weighted equally. However, in fitting the measured data to equations (9) and (10), we used a logarithmic scale for the dependent variable to increase the weighting on the smaller values of M_L.

Interpreting the Rate Constants

With reference to equation (5),

$$\frac{dM_X}{dt} = K_{XP}\,M_P - K_{PX}\,M_X,$$

it will be useful to represent the derivative dM_X/dt as the sum of 2 constituent derivatives, each greater than zero:

$$\frac{dM_X}{dt} = \left|\frac{dM_P}{dt}\right|_{P\to X} - \left|\frac{dM_X}{dt}\right|_{X\to P}. \tag{11}$$

The first derivative on the right-hand side of this equation governs transfer of TNF from plasma to compartment X, and the second derivative from compartment X to plasma. By comparing equations (5) and (11), we can write:

$$\left|\frac{dM_P}{dt}\right|_{P\to X} = K_{PX}\,M_P \tag{12}$$

and

$$\left|\frac{dM_X}{dt}\right|_{X\to P} = K_{PX}\,M_X. \tag{13}$$

Approximating the derivatives by finite differences, we have respectively:

$$\left|\frac{\Delta M_P/M_P}{\Delta t}\right|_{P\to X} = K_{XP}, \tag{14}$$

$$\left|\frac{\Delta M_X/M_X}{\Delta t}\right|_{X\to P} = K_{PX}. \tag{15}$$

Equation (15) permits us to interpret the rate constant K_{PX} as the fractional loss in TNF mass from the organ, X, per unit time. Hence, K_{PH} is the fractional loss in TNF mass from the heart per unit time, etc. The various values of K_{PX} for different organs can, therefore, be compared directly one with the other (Table 3). For liver and kidney, which exchange TNF with both plasma and an excreted pool (bile and urine, respectively), $K_{\Sigma L}$ and $K_{\Sigma R}$ are equal to the sum of 2 rate constants, as shown by equation (8). Since the values of the constituent rate constants are known, we can determine the fractional loss rate to both plasma and bile or plasma and urine.

Similarly, equation (14) allows the interpretation of K_{XP} as the fractional loss of TNF mass from the plasma per unit time, which is destined for the organ or tissue X. The sum of all the K_{XP}, as given in the first term on the right-hand side of equation (1), gives the total mass of TNF leaving plasma for peripheral tissues per unit time.

RESULTS

Weight Change of Animals

Surgical insertion of the cannula occurred on day 0 and subsequently the rats were allowed to recover for 5 days. During this time, animals were provided with liquid diet, which resulted in an average gain of approximately 3.6 g of body weight per day. After this recovery period, rats received a continuous infusion of physiologic saline through the central venous cannula in addition to the liquid diet resulting in a weight gain of approximately 3.4 g/d.

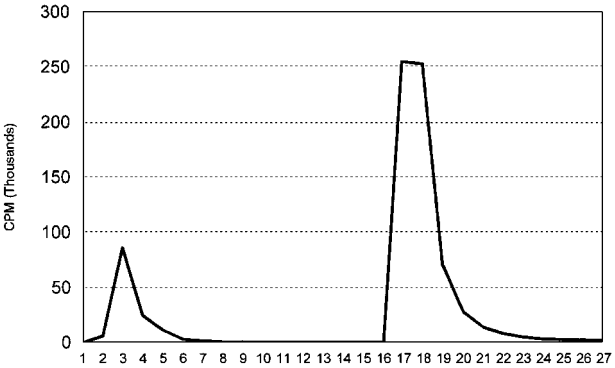

Fig 2. HPLC separation of native ^{125}I-TNF dissolved in saline on a C-4 protein column.

Proportion of Active ^{125}I-TNF in Samples

Precipitation of plasma samples resulted in a reduction in free ^{125}I by 82% (data not given). The HPLC separation of the native TNF (^{125}I-TNF in saline), as well as precipitated plasma samples, showed the presence of 2 peaks (Figs 2 and 3). SDS-PAGE of samples taken from the second peak showed the presence of bands representing TNF monomers, dimers, trimers, and tetramers (Fig 4). Therefore, we have shown that there is intact TNF present throughout the entire 3-hour experimental period. No bands were present after SDS-PAGE of any samples taken from the first HPLC peak, suggesting that this peak is a low molecular weight particle, such as free iodine or a small fragment of ^{125}I-TNF (Fig 4, lanes 2 and 4). HPLC separation of ^{125}I standard suggested that iodide eluted at the position of this first peak.

The proportion of the remaining first peak, which moves in the region of free ^{125}I, remained a constant proportion of the ^{125}I-TNF peak (58% of peak 2) at both the initial (time 0) and 3-hour time points. Because the proportion of the 2 peaks

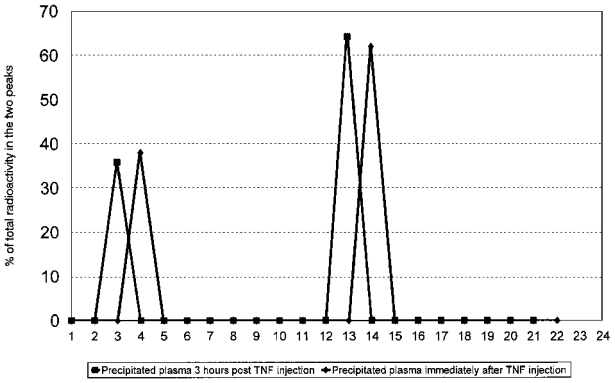

Fig 3. ^{125}I-TNF was injected into an experimental animal via a central venous cannula, and blood samples were withdrawn immediately after injection, as well as after 3 hours of circulation. Plasma collected at these 2 time points was precipitated with 15% TCA and the precipitates subjected to HPLC separation on a C-4 protein column. Two peaks were clearly visible: the first peak represents either free iodide or a low molecular weight fragment of ^{125}I-TNF, whereas the second peak represents ^{125}I-TNF. The radioactivity in each peak is presented as a percentage of the total in the 2 peaks and illustrates that the proportion of the radioactivity present in the first peak remains a constant proportion of that found in the second peak.

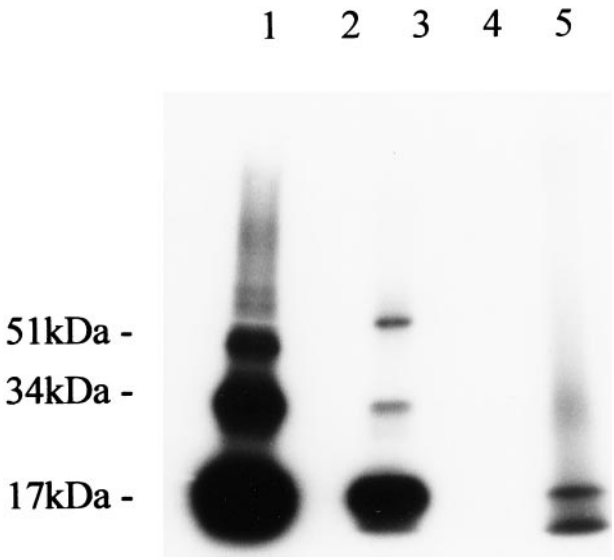

Fig 4. Gel electrophoresis of HPLC samples. Samples from each of the 2 HPLC peaks found on separation of (1) native ^{125}I-TNF (Fig 2); (2) precipitated plasma taken immediately post-TNF injection; and (3) precipitated plasma after 3 hours of circulation (Fig 3) were subjected to SDS-PAGE. Lane 1, native ^{125}I-TNF; lane 2, HPLC peak 1 native ^{125}I-TNF; lane 3, peak 2 native ^{125}I-TNF; lane 4, HPLC peak 1-3 hour precipitated plasma; lane 5, HPLC peak 2-3 hour precipitated plasma.

remained constant, it was unnecessary to correct each sample for the radioactivity present in this first peak (Fig 3).

Organ Uptake and Distribution of ^{125}I-TNF

The liver and kidney were found to take up the largest percentage of the injected dose followed by the lung and the intestine (Table 1). Initially, organ uptake (excluding skeletal muscle) accounted for approximately 20% of the injected dose. During the first 30 minutes post-TNF injection, approximately 63% of the injected dose was distributed between the blood and all compartments examined (Table 1). However, by the end of the 3-hour period, less than 10% of the TNF could be accounted for in the organs and the blood (excluding muscle). In an attempt to locate the remaining TNF, adipose tissue and skin were examined at the 3-hour time point in the rats used for the additional bile and urine experiment described above. These animals were found to have, on average, 50 g of skin and fur, which took up anywhere from 32% to 55% of the injected dose of TNF. Adipose tissue contained less than 0.7% of the injected dose of TNF at 3 hours suggesting that it is not a major site of TNF accumulation. Therefore, when the carcass and skin are considered together, these 2 sites would most likely account for the remaining part of the injected dose (Table 2). In addition, it is interesting to note that the TNF lost from the organs from 4 to 180 minutes can be largely accounted for by the cumulative loss of radioactivity into the bile and the urine.

Compartmental Modeling of TNF Distribution

A mammillary compartmental configuration was used to describe the interchange of TNF with the 10 organs and tissues measured (Fig 1). Using this model, we calculated the rate constants for the movement of TNF from the plasma to the organ, as well as from the organ back to the plasma (Table 3). The rate constant K_{XP} (where X is any organ) represents the fraction of the mass of TNF in the plasma that is going to tissue X per unit time. This rate constant may primarily reflect blood flow, but may also reflect the attraction of an organ for TNF. This rate constant has been corrected for the size of the organ thereby allowing direct comparison of this rate constant between tissues. On the other hand, the rate constant K_{PX} reflects the fraction of the mass of TNF in organ X, which is leaving the tissue to return to the plasma per unit time. This rate constant reflects what we will call the ''relative affinity'' or willingness of a tissue to hold onto TNF. Therefore, a tissue with a high affinity for TNF will hold onto TNF without destroying or releasing it.

Examination of the organ uptake of labelled TNF, as well as the rate constants for the movement of TNF, shows that tissues could be divided into 2 very distinct uptake patterns. The first type of pattern was found predominantly in muscle tissues (exclusive of the myocardium), which consist of a significant proportion of either smooth or striated muscle. These tissues show a slow but continuous accumulation of TNF throughout the 3-hour experimental period. These tissues have a small K_{PX} suggesting a high affinity for TNF of the organ (little fractional change in the mass of TNF within the organ) resulting in a net retention of TNF over time within this tissue (Table 3). In separate experiments, the mucosa from the stomach and several intestinal segments were separated from the muscular layer. These studies showed that >50% of the radioactivity measured in the intestinal tract (location independent) was associated with

Table 1. Total Organ Uptake of Labeled TNF as a Percent of the Injected Dose

	4 Minutes	10 Minutes	30 Minutes	60 Minutes	180 Minutes	Area Under Curve cpm/organ/180 Minutes
Liver	15.11 ± 1.68	11.96 ± 1.15	5.3 ± 0.73	3.77 ± 0.59	1.69 ± 0.18	718 ± 54
Kidney	2.61 ± 0.13	3.3 ± 0.18	2.80 ± 0.22	2.09 ± 0.21	0.58 ± 0.13	317 ± 18
Spleen	0.25 ± 0.11	0.30 ± 0.08	0.20 ± 0.10	0.30 ± 0.06	0.16 ± 0.07	44 ± 6
Stomach	0.06 ± 0.04	0.13 ± 0.04	0.20 ± 0.04	0.32 ± 0.07	0.49 ± 0.12	87 ± 12
Heart	0.54 ± 0.16	0.50 ± 0.10	0.31 ± 0.05	0.26 ± 0.04	0.094 ± 0.02	41 ± 3.9
Intestine	0.27 ± 0.27	0.35 ± 0.15	1.97 ± 0.47	1.25 ± 0.24	1.35 ± 0.32	258 ± 53
Lung	2.31 ± 0.32	2.37 ± 0.17	2.31 ± 0.58	1.7 ± 0.35	0.50 ± 0.06	256 ± 31
EDl	0.007 ± 0.006	0.007 ± 0.006	0.005 ± 0.002	0.04 ± 0.03	0.23 ± 0.008	5.9 ± 2.2
Soleus	0.003 ± 0.002	0.00	0.006 ± 0.003	0.01 ± 0.007	0.03 ± 0.007	4.9 ± 0.7
Diaphragm	0.23 ± 0.09	0.21 ± 0.04	0.1 ± 0.01	0.18 ± 0.04	0.09 ± 0.01	26 ± 3

NOTE. Data are expressed as the mean ± SEM.

Table 2. Uptake and Excretion of TNF as a Mean Percentage of the Injected Dose

	4 Minutes	10 Minutes	30 Minutes	60 Minutes	180 Minutes
Blood	42.51 ± 5.5	43.01 ± 4.2	20.06 ± 1.8	11.39 ± 1.6	3.38 ± 0.5
Organs	20.19 ± 2.2	19.15 ± 0.96	13.81 ± 1.24	9.51 ± 1.2	4.39 ± 0.67
Skin					50.5 ± 5
Skeletal muscle*	9.23 ± 9.13	9.63 ± 4.8	22.85 ± 6.1	22.33 ± 7.7	32.63 ± 5.5
Urine	0.03 ± 0.01	0.21 ± 0.14	0.42 ± 0.33	1.07 ± 0.67	3.54 ± 1.1
Bile	0.22 ± 0.01	0.4 ± 0.12	1.45 ± 0.2	2.67 ± 0.16	7.05 ± 1.6
Total	72.18	72.4	58.59	46.97	101

NOTE. Data are expressed as the mean ± SEM.
*Calculated based on the average amount of skeletal muscle per rat.[42]

the muscle layer with approximately 35% of the radioactivity being associated with the mucosa (data not shown).

In contrast, the visceral organs, the liver and the kidney, show a different pattern of TNF uptake and release. These organs have a rapid accumulation of TNF in the first 30 minutes of study followed by a rapid loss of TNF. The loss of TNF by these tissues may reflect the loss of intact TNF from the tissue or alternatively the release of radioactive iodide from the metabolism of TNF within these tissues. The finding that the cumulative loss of TNF from the tissues can be largely explained by the cumulative loss of TNF into the bile and urine supports the degradation of TNF within the visceral tissues. The rate constants for these tissues are large, suggesting both an increased fractional mass of plasma TNF is going to the visceral organs, as well as leaving the liver or kidney to go either back to the plasma or out into the bile or the urine. These rate constants represent a rapid initial accumulation of TNF within the visceral organs with little retention. Autoradiography of SDS gel-separated bile proteins support the presence of intact labeled TNF in the bile of experimental animals (Figs 5 and 6). Autoradiography of the separation of urine by gel electrophoresis failed to show the presence of any intact labeled TNF in the urine, suggesting that TNF is degraded within the kidney with the subsequent release of radioactive iodide.

DISCUSSION

Physiologically, TNF is produced in a burst in response to injury, trauma, or bacterial invasion and has been extensively linked to the metabolic alterations associated with sepsis or endotoxemia.[1,14] The production of TNF results in the activation of a cascade of endogenous and humoral mediators that modulate and amplify its effects.[1,14,15] Indeed, peak levels of circulating stress hormones, soluble TNF receptors, and other cytokines have been observed after peak levels of TNF have been achieved and continue to circulate long after TNF levels have become negligible.[14,16,17] Subsequently, TNF is cleared rapidly from the circulation resulting in relatively low or undetectable circulating levels.[3,4,6,14,16] This rapid clearance of TNF has made the interpretation of circulating levels of this cytokine in the clinical setting extremely difficult.

To simulate the physiologic burst of TNF that occurs during critical and chronic illness, we have studied the in vivo metabolism of a bolus of TNF to understand how the burst distributes itself. Studies of TNF metabolism have used combinations of labeled and unlabeled TNF. Classic studies by Beutler et al[3] showed that when an ''excess'' of unlabeled TNF was provided together with labelled TNF, there were only very slight changes in the TNF clearance patterns. This excess unlabeled TNF affected only the magnitude of TNF binding to tissues and not the relative magnitude of binding when each tissue was compared with the other. In fact, studies performed with or without the addition of cold TNF have found very similar patterns of TNF organ uptake at discrete time points, suggesting that these studies can be performed with or without the presence of unlabeled TNF.[3-6,14]

Experimental data on the plasma disappearance and tissue accumulation of TNF were used to create an in vivo model of TNF distribution over time in rats using a multicompartment

Table 3. Rate Constants for the Movement of TNF Between Tissues and Plasma

	K_{XP} (going to tissues from plasma)	K_{PX} (leaving tissues for plasma)
Intestine	0.044	**0.0098**
Lung	1.94	0.13
Liver	18.21	1.83
Spleen	0.32	0.09
Diaphragm	1.03	0.50
EDL	0.047	**0.003**
Soleus	0.008	**0.004**
Kidney	2.37	0.13
Stomach	0.03	**0.02**
Heart	1.57	0.43

NOTE. The rate constant K has the units of time^{-1}.
Abbreviation: EDL, extensor digitorum longus.

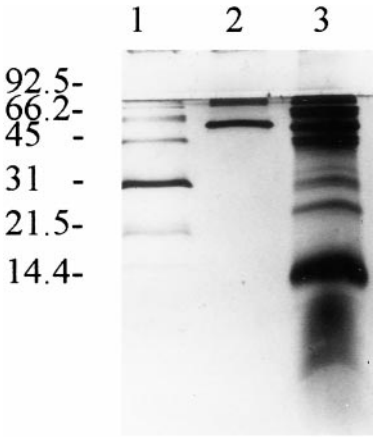

Fig 5. SDS-PAGE of bile samples under reducing conditions. Lane 1, low molecular weight markers; lane 2, labeled TNF; and lane 3, bile sample.

Fig 6. Autoradiograph of the gel in Fig 5 after 7 weeks of exposure. Lane 1, bile sample; lane, 2 labeled TNF; and lane 3, low molecular weight markers. Bands representing the presence of intact TNF were seen in the bile of the experimental animals.

model. Previously, the organ uptake of TNF had been studied only at isolated time points with little integration of the uptake to other tissues or to the plasma disappearance of TNF.[3,4,5,6,14] The patterns of tissue accumulation and loss of TNF will largely reflect the balance between TNF binding to cell surface and soluble TNF receptors. Proteolytic cleavage of the extracellular domain of the 2 TNF cell surface receptors results in the production of soluble TNF receptors, which remain able to bind TNF in the circulation.[2,18] These receptors have been shown to act both as TNF antagonists by binding TNF and preventing its interaction with cell surface receptors and as reservoirs of bioactive TNF by stabilizing its tertiary structure and allowing it to be slowly released.[19,20] Levels of soluble TNF receptors are present in the serum of normal humans and become elevated during a variety of inflammatory and noninflammatory diseases.[21,22] The factors that trigger the release of these receptors are unknown. Our model is unique in that it allows an integration of the patterns of TNF uptake and loss by tissues with the production of soluble TNF receptors. These soluble TNF receptors will ultimately affect the balance between circulating levels of TNF and the binding and distribution patterns of TNF to tissues. In addition to the determination of the major sites of TNF accumulation and loss in vivo, these studies describe, for the first time, 2 distinct patterns of TNF uptake, which may reflect the physiologic actions of TNF at these sites.

In the visceral organs, the large K_{XP} may simply reflect increased blood flow to these organs, but may also suggest an increased number of TNF receptors or an increased binding strength for TNF by existing receptors. The net result is a strong initial attraction for TNF leading to a large fraction of the mass of TNF in the plasma going to these tissues. However, these tissues also have a large K_{PX} suggesting that there is also a large fraction of the mass of TNF that is leaving these tissues. The loss of TNF from these tissues is similar to the cumulative loss of TNF into the bile and urine, suggesting that the TNF lost from these tissues is at least partially degraded and released as radioactive iodide into the urine. This pattern of rapid uptake and loss suggests that it is tissues with this type of uptake pattern that are primarily responsible for TNF metabolism. Furthermore, the release of TNF into the bile and the urine supports earlier studies, which have concluded that the kidney and the liver are the organs primarily associated with TNF clearance.[3,4,23] In addition, studies of TNF kinetics have shown that TNF clearance is impaired in nephrectomized animals in comparison with control animals, supporting the importance of the kidney in TNF metabolism.[4,24] Radioactivity measured in the urine was not associated with intact TNF suggesting that the kidney metabolizes TNF with a subsequent release of free iodide into the urine.

In contrast, the muscle tissues, (exclusive of the myocardium) such as the EDL, soleus, the stomach, and the intestine, which consist of a significant proportion of either smooth or striated muscle, showed a second distinct pattern of TNF accumulation and loss. These tissues followed a pattern of slow and continuous TNF accumulation over the entire 3-hour period. In addition, the extremely small K_{PX} for these tissues indicates that these tissues have a very high affinity for TNF and release very little back to the plasma resulting in a sequestration of TNF within these tissues.

While it is relatively clear that a pattern of rapid TNF accumulation and loss reflects tissues primarily responsible with the metabolism of TNF, it is less clear the relationship between muscle sequestration of TNF and the physiologic action of TNF on muscle. The production of TNF has been linked with the development of anorexia, as well as with the accelerated wasting of peripheral muscle proteins. The chronic administration of TNF in humans and animals resulted in decreased food intake and weight loss, the severity of which may be related to the site of TNF production.[25-27] Treatment of animals with anticachectin/anti-TNF antibodies was found to attenuate the anorexia and weight loss associated with multiple injections of recombinant TNF or in animals with transplantable tumors.[28,29] TNF has been found to affect gastric emptying and motility, which contribute to the development of anorexia.[30,31] Wasting of the muscular layer of the intestine may result in impaired motility and impaired gastric emptying, thereby contributing to the anorexic response during illness. Our finding of increased TNF accumulation in the intestine and stomach of animals suggests that TNF binding to these tissues may affect their function.

In addition to contributing to the development of anorexia, TNF has been linked to the accelerated wasting of peripheral muscle observed in critical illness. In critical and chronic illness, there is a marked wasting of skeletal muscle with a relative preservation or even enhanced protein content, DNA, and RNA of the viscera.[15,32] This enhanced visceral protein content is believed to contribute to the production of acute phase reactants, as well as for the synthesis of glucose.[29] The finding of a slow, but continuous, uptake of TNF by the peripheral muscles (EDL and soleus) suggests that TNF binding and sequestration by peripheral muscle tissue could mediate tissue wasting. The wasting of peripheral muscle may also contribute to the respiratory failure observed in critically ill patients. The link between TNF retention and tissue wasting is strengthened by the observation that tissues showing little TNF retention, such as the liver, do not become wasted when TNF is present.[15]

The pattern of TNF retention in peripheral muscle tissues suggests that TNF may also bind to and be retained by the smooth muscle cells lining the blood vessel walls. The accumulation of TNF may mediate the wasting of these muscles resulting in the decreased peripheral vascular resistance and the hemodynamic collapse associated with TNF administration. TNF administration to animals and humans results in a dramatic drop in cardiac output, hypotension, and decreased peripheral vascular resistance. Therapeutic trials designed to determine dosing schedules of human recombinant TNF for use in cancer patients were limited due to the development of hypotension.[33] TNF given to rats, beagles, or baboons resulted in hypotension, tachycardia, tachypnea, and respiratory failure.[27,34] These findings were associated with depressed blood pressure, cardiac output, vascular resistance, and impaired left ventricular ejection fraction, which lasted for days after TNF administration in dogs.[35] These findings are identical to those of septic shock. In addition, the pretreatment of baboons with anti-TNF monoclonal antibody (MoAb) protected the animals against the hemodynamic collapse and death seen in the untreated animals given TNF even though bacteremia was present.[36] Studies by Amrani et al[37] found in second to fourth order rat cremaster muscle arterioles that acute exposure to TNF resulted in significant dilatation, which was not observed when arterioles were pretreated with TNF neutralizing antibodies. Research has now focussed on the role of TNF in the induction of nitric oxide synthase (iNOS) by smooth muscle cells. Studies have suggested that TNF and other cytokines can induce nitric oxide synthesis in smooth muscle cells resulting in the vasodilatation and hypotension seen in septic shock.[38] In addition, Baudry et al[39,40] showed that tracheal smooth muscle cells (TSMC) expressed both the p-55 and p-75 TNF receptors, and that binding of TNF to the p-55 receptor resulted in changes in calcium homeostasis, as well as in TSMC growth. These investigators concluded that the binding of TNF could modulate smooth muscle cell function, and that the action of TNF at each receptor would be tissue-dependent.[39,40] Therefore, there is evidence that the binding of TNF to smooth muscle cells in the blood vessel wall may be a key factor in the regulation of blood pressure during illness.

There are some caveats; while most tissues bind TNF, binding alone does not appear to be the sole factor responsible for the biologic effects of TNF.[41] Neither TNF receptor number nor the relative strength of binding has been linked to the susceptibility of a tissue to cytotoxicity or to TNF-stimulated growth. In addition, the pathways by which each TNF receptor signals its biologic responses are also relatively unknown. Finally, the physiologic significance of TNF binding to soluble TNF receptors remains to be proven, as well as the factors that affect the relative distribution of cell surface and soluble TNF binding proteins. Therefore, the binding of TNF to tissues reflects a complex interplay between soluble and cell surface TNF receptors, which may significantly affect the nature or the magnitude of the physiologic response to TNF at the tissues. This study represents the first attempt to create an in vivo model of TNF distribution between the plasma and the tissue compartments and will lead to further studies using molecular techniques to link the tissue uptake of TNF to the biologic effects of TNF.

ACKNOWLEDGMENT

We acknowledge the contributions of R. Kurian, Dr N. Raina, and the laboratory of Dr D. Osborne.

REFERENCES

1. Fong Y, Moldawer LL, Shires T, et al: The biologic characteristics of cytokines and their implication in surgical injury. Surg Gynecol Obstet 170:363-378, 1990

2. Pennica D, Kohr WJ, Fendly BM, et al: Characterization of a recombinant extracellular domain of the type 1 tumor necrosis factor receptor: Evidence for tumor necrosis factor-α induced receptor aggregation. Biochemistry 31:1134-1141, 1992

3. Beutler BA, Milsark I, Cerami A: Cachectin/tumor necrosis factor: Production, distribution and metabolic fate in vivo. J Immunol 135:3972-3977, 1985

4. Ferraiolo BL, McCabe J, Hollenbach S, et al: Pharmacokinetics of recombinant human tumor necrosis factor-α in rats: Effects of size and number of doses and nephrectomy. Drug Metab Dispos 17:369-372, 1989

5. Keith ME, Norwich KH, Jeejeebhoy KN: Nutrition support affects the distribution and organ uptake of cachectin/tumor necrosis factor in rats. JPEN 19:341-350, 1995

6. Pang X, Hersham JM, Pekary AE: Plasma disappearance and organ distribution of recombinant human tumor necrosis factor in rats. Lymphokine Cytokine Res 10:301-306, 1991

7. Popp MB, Brennan MF: Long term vascular access in the rat: The importance of asepsis. Am J Physiol 241:H606-612, 1981

8. Matsui J, Cameron RG, Kurian R, et al: Nutritional, hepatic, and metabolic effects of cachectin/tumor necrosis factor in rats receiving total parenteral nutrition. Gastroenterology 104:235-243, 1993

9. Gutierrez EG, Banks WA, Kastin AJ: Murine tumor necrosis factor alpha is transported from blood to brain in the mouse. J Neuroimmunol 47:169-176, 1993

10. Laemmli UK: Cleavage of structural proteins during the assembly of the head of bacteriophage T4. Nature 227:680-685, 1970

11. Raina N, LaMarre J, Liew CC, et al: Effect of nutrition on tumor necrosis factor receptors in weight gaining and losing rats. Am J Physiol 277:E464-E473, 1999

12. Sterling K, Gray SJ: Determination of the circulating red cell volume in man by radioactive chromium. J Clin Invest 29:1614-1619, 1950

13. Schagger H, von Jagow G: Tricine-sodium dodecyl sulfate-polyacrylamide gel electrophoresis for the separation of proteins in the range from 1 to 100 kDa. Anal Biochem 166:360-379, 1987

14. Hesse DG, Tracey KJ, Fong Y, et al: Cytokine appearance in human endotoxemia and primate bacteremia. Surg Gynecol Obstet 166:147-153, 1988

15. Fong Y, Lowry SF, Cerami A: Cachectin/TNF: A macrophage protein that induces cachexia and shock. JPEN 12:072S-077S, 1988

16. Lantz M, Malik S, Slevin ML, et al: Infusion of tumor necrosis factor (TNF) causes an increase in circulating TNF-binding proteins in humans. Cytokine 6:402-406, 1990

17. Van Zee KJ, Kohno T, Fischer E, et al: Tumor necrosis factor soluble receptors circulate during experimental and clinical inflammation and can protect against excessive tumor necrosis factor-α in vitro and in vivo. Proc Natl Acad Sci USA 89:4845-4849, 1992

18. Fernandez-Botran R: Soluble cytokine receptors: Their role in immunoregulation. FASEB J 5:2567-2574, 1991

19. Aderka D, Engelmann H, Maor Y, et al: Stabilization of the bioactivity of tumor necrosis factor by its soluble receptors. J Exp Med 175:323-329, 1992

20. Hale KK, Smith CG, Baker SL, et al: Multifunctional regulation of the biological effects of TNF-α by the soluble type I and type II TNF receptors. Cytokine 7:26-38, 1995

21. Aderka D, Engelmann H, Hornik V, et al: Increased serum levels of soluble receptors for tumor necrosis factor in cancer patients. Cancer Res 51:5602-5607, 1991

22. Barak V: Soluble cytokine receptors in disease. Isr J Med Sci 31:565-571, 1995

23. Pessina GP, Pacini A, Bocci V, et al: Studies on tumor necrosis factor (TNF):II. Metabolic fate and distribution of human recombinant TNF. Lymphokine Res 6:35-44, 1987

24. Bemelmans MHA, Gouma DJ, Buurman WA: Influence of nephrectomy on tumor nerosis factor clearance in a murine model. J Immunol 150:2007-2017, 1993

25. Darling G, Fraker DL, Jensen C, et al: Cachectic effects of recombinant human tumor necrosis factor in rats. Cancer Res 50:4008-4013, 1990

26. Sherman ML, Spriggs DR, Arthur KA, et al: Recombinant human tumor necrosis factor administration as a five-day continuous infusion in cancer patients: Phase I toxicity and effects on lipid metabolism. J Clin Oncol 6:344-350, 1988

27. Tracey KJ, Morgello S, Koplin B, et al: Metabolic effects of cachectin/tumor necrosis factor are modified by site of production. J Clin Invest 86:2014-2024, 1990

28. Sherry BA, Gelin J, Fong Y, et al: Anticachectin/tumor necrosis factor-alpha antibodies attenuate development of cachexia in tumor models. FASEB J 3:1956-1962, 1989

29. Tracey KJ, Wei H, Manogue R, et al: Cachectin/tumor necrosis factor induces cachexia, anemia and inflammation. J Exp Med 167:1211-1227, 1988

30. Patton JS, Peters J, McCabe J, et al: Development of partial tolerance to the gastrointestinal effects of high doses of recombinant tumor necrosis factor-alpha. J Clin Invest 80:1587-1596, 1987

31. Tracey KJ, Beutler B, Lowry SF, et al: Shock and tissue injury induced by recombinant human cachectin. Science 234:470-474, 1986

32. Kinney JM, Elwyn DH: Protein metabolism in injury. Annu Rev Nutr 3:433-466, 1983

33. Creaven PJ, Plager JE, Dupere S, et al: Phase I clinical trial of recombinant human tumor necrosis factor in patients with advanced solid tumors. Cancer Chemother Pharmacol 20:137-144, 1987

34. Tracey KJ, Lowry SF, Fahey TJ, et al: Cachectin/tumor necrosis factor induces lethal shock and stress hormone responses in the dog. Surg Gynecol Obstet 164:415-422, 1987

35. Natanson C, Eichenholz PW, Danner RL, et al: Endotoxin and tumor necrosis factor challenge in dogs stimulate the cardiovascular profile of human septic shock. J Exp Med 169:823-832, 1989

36. Tracey KJ, Fong Y, Hesse DG, et al: Anti-cachectin/TNF monoclonal antibodies prevent septic shock during lethal bacteremia. Nature 330:662-664, 1987

37. Amrani Y, Panettieri RA Jr, Frossard N, et al: Activation of the TNFα-p55 receptor induces myocyte proliferation and modulates agonist evoked calcium transients in cultured human tracheal smooth muscle cells. Am J Respir Cell Mol Biol 15:55-63, 1996

38. Kuemmerle JF: Synergistic regulation of NOS II expression by IL-1β in cultured rat colonic smooth muscle cells. Am J Physiol 274:G178-G185, 1998

39. Baudry N, Rasetti C, Vicaut E: Differences between cytokine effects in the microcirculation of the rat. Am J Physiol 71:H1186-H1192, 1996

40. Baudry N, Vicaut E: Role of nitric oxide in effects of tumor necrosis factor-α on microcirculation in the rat. J Appl Physiol 75:2392-2399, 1993

41. Yoshie O, Tada K, Ishida N: Binding and crosslinking of ^{125}I-Labelled recombinant human tumor necrosis factor to cell surface receptors. J Biochem 100:531-541, 1986

42. Munro HN: Evolution of protein metabolism, in Munro HN (ed): Mammalian Protein Metabolism. New York, NY, Academic, 1969, p 153